Powder Technology 329 (2018) 95–106

Contents lists available at ScienceDirect

Powder Technology

journal homepage: www.elsevier.com/locate/powtec

In-situ synthesis and characterization of nano-structured NiAl-Al_2O_3 composite during high energy ball milling

Maryam Beyhaghi [a,*], Jalil Vahdati Khaki [b], Maykel Manawan [c,d], Alireza Kiani-Rashid [b], Mehrdad Kashefi [b], Stefan Jonsson [e]

[a] Department of Metallurgy and Ceramics, Faculty of Engineering, Mashhad Branch, Islamic Azad University, Mashhad, Iran
[b] Department of Metallurgical and Materials Engineering, Ferdowsi University of Mashhad, 91775-1111 Mashhad, Iran
[c] Department of Physics, Universitas Indonesia, Depok 16424, Indonesia
[d] Energy Engineering, Politeknik Negeri Jakarta, Depok 1624, Indonesia
[e] Department of Materials Science and Engineering, Royal Institute of Technology, SE-10044 Stockholm, Sweden

ARTICLE INFO

Article history:
Received 23 September 2017
Received in revised form 14 January 2018
Accepted 20 January 2018
Available online 02 February 2018

Keywords:
Composite
Nanostructured
Mechanosynthesis
Ball mill
NiAl
Al_2O_3

ABSTRACT

In this work, synthesis of NiAl–Al_2O_3 nanocomposite powders via the mechanosynthesis route and by using Ni, NiO and Al is investigated. Ignition of the reaction inside the ball-mill vial happens after 110 min; NiO is totally finished and NiAl and Al_2O_3 as product phases are formed. After 10 h of ball milling, raw materials are totally used in the reaction and only product phases exist in the vial. By continuing the ball milling process to 60 h, better mixing of the synthesized phases and decrement in their crystallite sizes plus particle size are observed. Crystallite sizes of the product phases are in the nanometer range in all ball milling times. Crystallite sizes of NiAl and Al_2O_3 after 10 h are around 11 nm and 19 nm respectively, and these are reduced to around 8 nm for both phases after 60 h of ball milling.

1. Introduction

Mechanical energy has been proved capable of providing the energy needed to start a reaction as well as thermal energy. It is reported that high energy ball milling provides energy for activation of a chemical reaction [1–4] and also for full occurrence of a chemical reaction [5,6] during milling. The first is defined as mechanical activation and the second is called as mechanochemical synthesis or reactive milling. In such a process, the intensely high mechanical impacts result in repeated welding and fracturing of powder particles. Therefore, the contact area between the reactant powder particles increases and fresh surfaces come into contact in each collision in the ball mill. This matter leads the reaction to proceed without the necessity for diffusion through the product layer. Intense plastic deformation, increment in strain energy and thus high defect density leads to activation/occurrence of a chemical reaction. High defect density accelerates the diffusion process during mechanical milling [7,8].

Hence, it is expected that kinetic and thermodynamic behavior of the aforementioned reactions may be very different from those reactions initiated by thermal energy.

These reactions might undergo two different kinetics based on milling conditions:

1- Gradual reactions or progressive type reactions in which materials transform in a gradual manner and in very small volumes during each collision.

2- A self-propagating combustion reaction when the reaction enthalpy is high enough [8,9].

In the latter type, there is a critical milling time in which the combustion reaction initiates. In the beginning, the temperature of the milling vial shows a slow increase over time. Then, it increases abruptly which implies that the reaction ignition has occurred (ignition time = t_{ig}). After this time, temperature decreases slowly. Measurement of t_{ig} enables definition of the structural and chemical evolution during combustion reaction [10].

In the reactive milling method, there are varied and numerous benefits and these make this process economical. These benefits include the ability to produce solid solutions [11], different volume fractions of different types of submicron reinforcements [12,13] as well as nascent clean interfaces [14]. Researchers have focused on intermetallics such as nickel aluminides. They utilize advantages of this process to improve ductility of such materials by microstructure refinements and to enhance their creep resistance by the reinforced particulates [15]. These goals have led researchers to concentrate on nanostructured composites.

* Corresponding author.
E-mail address: Beyhaghi@mshdiau.ac.ir (M. Beyhaghi).

https://doi.org/10.1016/j.powtec.2018.01.052
0032-5910/

Alumina has been considered as a promising reinforcement for NiAl by researchers [16,17]. That is because of its thermodynamic compatibility with NiAl and also because its thermal expansion coefficient is relatively close to that of NiAl. And furthermore, alumina has desirable properties such as low density, high specific strength, high modulus and good oxidation resistance [18]. Research has shown that NiAl–Al_2O_3 composite can be utilized for high temperature applications because of improved oxidation [19] and creep resistance [20] and thus is a good candidate for coating purposes [21].

Researchers have reported the formation of NiAl–Al_2O_3 composites by mechanical milling powder mixtures of Ni, Al and Al_2O_3 [22], NiO and Al [23] and $Ni_2(OH)_2CO_3 \cdot 3H_2O$ and Al [24]. Anvari et al. [25] developed NiAl-Al_2O_3 composite by high-energy ball milling of Ni, NiO and Al in a planetary ball mill without any process controlling agent (PCA). Udhayabanu et al. [26] carried out reactive milling of Ni, NiO and Al powder mixture in toluene medium. Then they heated the as-milled powder. Even after the 20 h of ball milling, reaction between raw materials was still incomplete; significant amounts of Ni and NiO remained in the mixture and Al was totally consumed. NiAl-Al_2O_3 composite was gained after the mixture was heated to 1200 °C. Udhayabanu et al. [15] consolidated the as-milled powder containing NiAl, amorphous Al_2O_3 and unreacted NiO by spark plasma sintering and finally gained NiAl-Al_2O_3 composite. Because the above-mentioned researchers have conducted their milling in conditions different from the present work, the phase formation and reaction mechanism are expected to be different in this study.

The present research aims to develop NiAl-Al_2O_3 nano-structured composite by reactive milling of Ni, NiO and Al as raw materials and by completing the reaction totally in the ball mill vial. Ignition time of the reaction is measured. Influence of ball milling time is assessed on phase evolution, crystallite size and lattice strain of phases, microstructure and chemical composition of different phases in the as-milled powder mixture and powder particle size (for milling times higher than 10 h).

2. Experimental

2.1. Characterization

Ball milling was carried out in a Retsch planetary ball mill. The constant ball milling conditions are mentioned in Table 1 and only ball milling time differs for different samples.

Starting powders were weighed into stoichiometric composition corresponding to Eq. (1):

$$3NiO + 8Ni + 13Al = Al_2O_3 + 11NiAl \quad (1)$$

Stearic acid (1 wt% of the powder mixture) was used as process controlling agent (PCA) to avoid oxidation and excessive cold welding of powders to vial and balls.

Temperature variations of outer wall of the ball mill vial were studied as an indirect indicator of the temperature changes inside the vial. For this purpose, two RoHS Thermochromic Liquid Crystal Reversible Temperature Indicating Strips were attached on the outer wall of the vial. In these strips, temperature ranges are seen in dark brown squares and color change of one square from brown to green indicates temperature change to that range. The temperature range under this survey was 60 °C. This assessment was intended to determine the ignition time of the exothermic reaction inside the ball mill vial.

Table 1
The ball milling conditions.

Vial	Stainless steel vial with volume of 250 ml
Balls	WC balls with approximate weight of 8.4 g/ball
Ball milling speed (rpm)	280
ball-to-powder ratio	10/1
Process controlling agent (PCA)	Stearic acid (1 wt% of the powder mixture)
Raw materials powder mixture weight (g)	Total weight: 5.85 (Ni:2.63, NiO:1.25, Al:1.97)
Ball milling time (h)	1, 2, 3, 4.5, 6, 10, 15, 20, 40, 60
Ball milling atmosphere	Air

The morphologies, microstructures and chemical compositions were studied using a LEO 1530 scanning electron microscope (SEM) with a Gemini column and EDS detector from Oxford Instruments of type 50 mm^2 XMax Silicon Drift Detector (SDD). To prepare samples for powder morphology investigations, powder particles were dispersed in ethanol. To study the microstructure of powder particles and phase investigations, a powder particle cross-section sample was prepared by conventional metallographic techniques. Phase evolution of samples was analyzed by PANalytical X'pert PRO XRD, using Cu Kα radiation with $\lambda = 0.15406$ nm. Using diffraction data of ball milled powder samples, the amount, crystallite size and lattice strain of existing phases were obtained from Rietveld refinement analysis by applying a pseudo-Voigt function and by X'Pert HighScore Plus software. The particle size measurement of raw materials and powder samples was performed using a SHIMADZU SALD-2101 apparatus.

2.2. Materials

Raw-materials used in this work were Al (Merck-art no.1056), Ni (Merck-art no.12277) and NiO (Merck-art no.6723) powders. Particle size measurement showed that d50 of Al, Ni and NiO was 68 ± 0.5, 5 ± 0.1 and 9 ± 0.3 μm, respectively. Fig. 1 shows scanning electron microscopy micrographs of the starting powder particles. The aluminum and nickel powder particles had spherical morphologies while nickel oxide powder particles showed an irregular shape.

3. Results and discussion

3.1. Phase analyses

Fig. 2 presents XRD patterns of the mixed powder mixture (0 h of high energy ball milling) and ball milled ones after different milling times. In the mixed and 1 h ball milled powder, peaks of Ni, Al and NiO are observed, so these were just reactant phases and none of reaction products were formed in powders. While increasing milling time to 2 h led to the disappearance of NiO peaks, NiAl and Al_2O_3 peaks began to appear, which are formed "in-situ" during the milling process. It should be mentioned that in the binary phase diagram of NiO-Al_2O_3, there is no complex oxide composition other than $NiAl_2O_4$ and peaks of this phase were not observed in any of patterns in Fig. 2. Thus, knowing that ball milling is not an equilibrium process, it seems that NiO is not consumed in any complex oxide in Ni-Al-O system and that Al_2O_3 is the product of reduction reaction of NiO and Al. Therefore, within 1 and 2 h of ball milling, the exothermic reaction between starting powders has taken place. With further milling, the intensity of Al and Ni peaks decreases. After 4.5 h of ball milling, Al peaks are not observable in XRD pattern while Ni peaks can still be seen. This has been reported in other references too. Peak broadening is a common phenomenon which is observed as a result of grain refinement and increase in lattice strain [5,27]. Because of the high ductility of aluminum in comparison with Ni, it experiences rapid and severe deformation. Therefore, the broadening and disappearing of peaks happens faster for aluminum, while nickel diffraction lines are observable over longer times because of its greater hardness and so undergoes less deformation than aluminum. Abbasi et al. [28] observed the same phenomenon in milling of nickel and aluminum powder mixture. If solid solution of Ni(Al) forms during ball milling, because of radius difference between nickel and aluminum, it is expected that expansion in the nickel lattice happens and thus Ni diffraction peaks should be detected at lower 2θ. But since such a peak shift is not seen in phase analysis results, it can be concluded that Ni(Al) solid solution has not been formed during

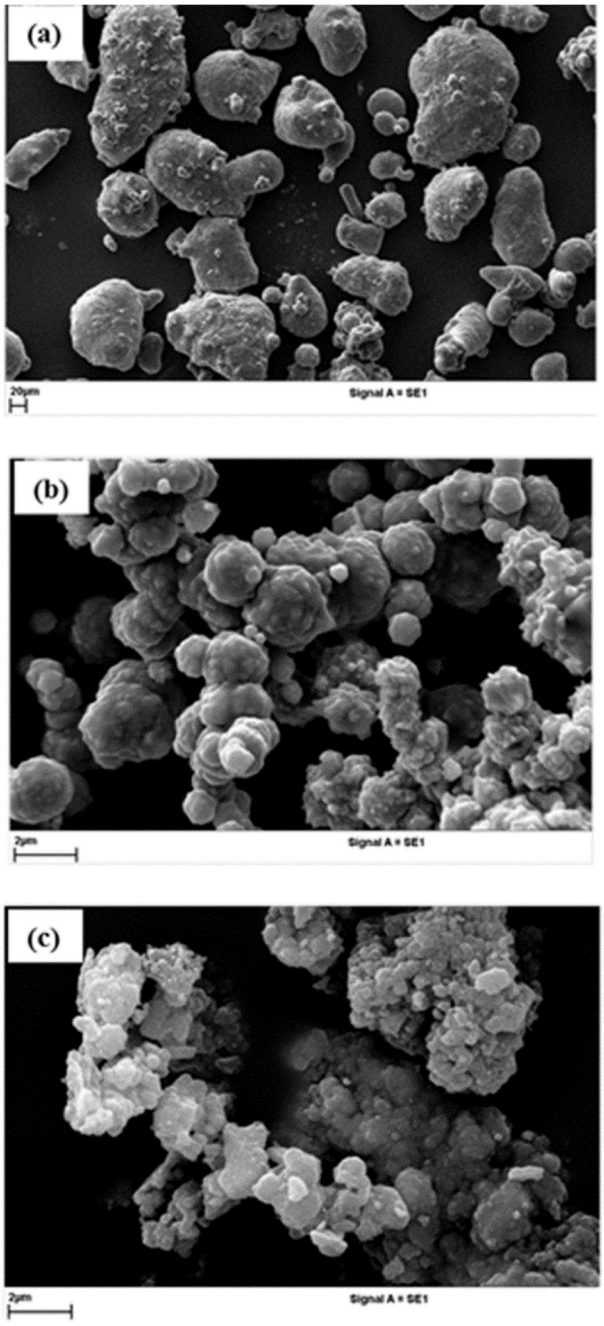

Fig. 1. SEM micrographs of starting powder particles: (a) Al, (b) Ni and (c) NiO.

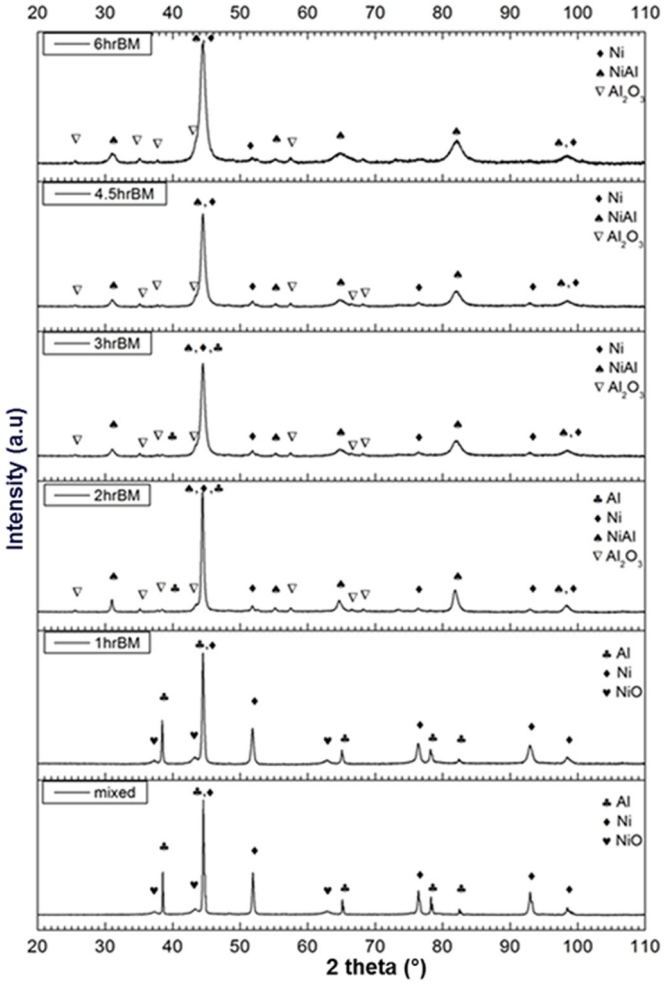

Fig. 2. XRD patterns of powder samples ball milled for 0 to 6 h. Observation of peaks of product phases after 2 h of ball milling, peak intensity weakening for starting materials with progression in milling.

milling. Studies on heating of the nickel aluminum binary system demonstrated that the phase formation sequence is $NiAl_3/Ni_2Al_3/NiAl/Ni_3Al$ [29,30]. However, in XRD patterns of ball milled powder, the only formed nickel aluminide phase is NiAl. In reactive milling, mechanical energy is employed to initiate chemical reactions. Intense mechanical pressure in ball milling causes formation of new surfaces, plastic deformation and increase in lattice defect density which makes the kinetics and thermodynamics of reactions in ball milling very different from that of thermally activated reactions. Ball milling leads to particle refinement and thus reduction in diffusion distances (by reduction in interlamellar spacing) which lowers the activation energy for diffusion significantly [8,26,28]. During milling, the system temperature is more or less constant and around room temperature. However, intense pressure is imparted drastically on powder particles by balls and the vial wall. By increment in pressure, according to Eq. (2), the system proceeds towards decrement in volume or increment in density.

$$\left[\frac{d\Delta G}{dP}\right] = \Delta V \tag{2}$$

In Eq. (2), variations of Gibbs free energy between the pressure of 1 atm and the imparted pressure on powder particles by ball impacts should be considered. As mentioned, in a ball milling system the activation energy for the required reactions to occur is obtained from mechanical energy rather than from thermal energy. Therefore, in such a system, the highest probability of formation belongs to a phase for which formation reaction results in a higher extent of volume reduction [31]. In Table 2, calculation of normalized volume reduction percentage in the formation reaction of different nickel-aluminides in Ni-Al system is reported.

According to Table 2, the formation reaction of NiAl causes the highest volume reduction, so NiAl is the only phase which is expected to form in the system. Researchers have also observed formation of the only phase of NiAl in powder system with stoichiometric composition of Ni50-Al50 [35–37].

Phase analysis results for powders ball milled for 10 h and more is demonstrated in Fig. 3. It is observed that after 10 h of ball milling, just two product phases of NiAl and Al_2O_3 exist in the system. As the milling progresses, only peak broadening of phases is seen in XRD patterns. The aim of continuation of milling for more than 10 h is to

Table 2
Volume reduction percentage in the formation reaction of different nickel-aluminide phases.

Phase	Density (g/cm^3)	Formation reaction	Normalized volume reduction percentage in the formation reaction
$NiAl_3$	3.95 [32]	$Ni + 3Al = NiAl_3$	$(\Delta V/V_0)\% = (V_{NiAl3}\text{-}3V_{Al}\text{-}V_{Ni}) / (3V_{Al} + V_{Ni}) * 100 = -3.34$
Ni_2Al_3	4.76 [32]	$2Ni + 3Al = Ni_2Al_3$	$(\Delta V/V_0)\% = (V_{Ni2Al3}\text{-}3V_{Al}\text{-}2V_{Ni}) / (3V_{Al} + 2V_{Ni}) * 100 = -3.48$
NiAl	5.85 [33]	$Ni + Al = NiAl$	$(\Delta V/V_0)\% = (V_{NiAl}\text{-}V_{Al}\text{-}V_{Ni}) / (V_{Al} + V_{Ni}) * 100 = -11.71$
Ni_3Al	7.26 [34]	$3Ni + Al = Ni_3Al$	$(\Delta V/V_0)\% = (V_{Ni3Al}\text{-}V_{Al}\text{-}3V_{Ni}) / (V_{Al} + 3V_{Ni}) * 100 = -6.07$

achieve uniform distribution of phases in powder particles. In addition to refinement of crystallites and increment in lattice strain, the lower intensity of alumina peaks than that with NiAl ones is because of the lower atomic scattering factor of Al_2O_3 than NiAl. The atomic scattering factor is proportional to atomic number in a phase. The higher the atomic scattering factor of a phase is, the sharper and more distinguishable the peaks are. The material with lower atomic scattering factor shows peaks with lower intensity and, in longer ball milling times, these peaks diminish. It seems that the atomic scattering factor is very important in affecting peak intensity [8]. In other works, researchers faced the same problem in defining alumina peaks properly in XRD patterns. In a work by Marashi et al. [38] in WC-Al_2O_3 system, despite the existence of 34.24 wt% of alumina, alumina peaks could not be distinguished even after 2 h of milling. Hosseinpour et al. [39] in Mo-ZnS system in presence of alumina, could not observe alumina peaks in XRD patterns, although they had 26 wt% of alumina in their system.

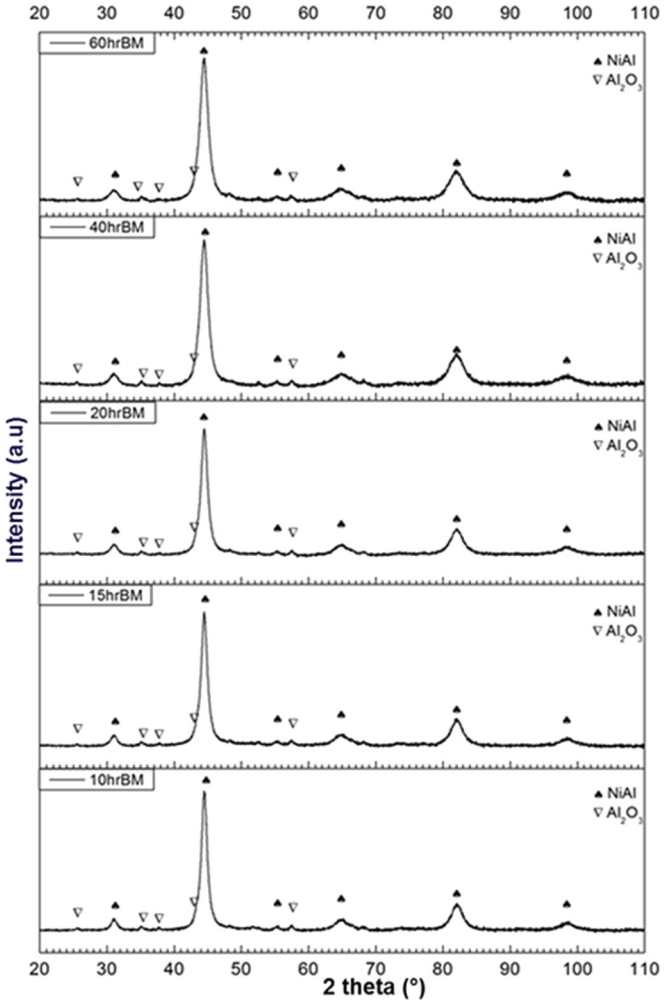

Fig. 3. XRD patterns of powder samples ball milled for 10 to 60 h. Observation of only product phases peaks after 10 h of ball milling, peak broadening with milling prolongation.

3.2. Finding ignition time (t_{ig}) in ball mill

According to phase analysis results in Fig. 2, after ball milling for 1 h only starting materials exist in the system, while in sample ball milled for 2 h, products began to appear. Therefore, it is expected that the reaction between raw materials has happened between 1 and 2 h of ball milling. To find the ignition time of the exothermic reaction, RoHS Thermochromic Liquid Crystal Reversible Temperature Indicating Strips are used as explained in Section 2.1. For this purpose, the ball mill was turned off every ten minutes and the temperature of the vial wall was recorded. It should be mentioned that before starting the ball milling process, the temperature indicating strips showed 20 °C as the wall temperature. The wall temperature was 30 °C after 60, 70, 80, 90 and 100 min of milling, indicated by the temperature indicating strips. But, after 110 min of milling, the wall temperature increased abruptly and the temperature indicating strip showed a sudden 5 °C increase. So, it is concluded that an exothermic reaction has happened between 100 and 110 min of ball milling and caused the temperature of the vial wall to increase.

In Fig. 4, phase diffraction lines for powder ball milled for 110 min are reported. Peak positions for identified phases by X'Pert High Score Plus software are also reported. As can be observed, product phases of NiAl and Al_2O_3 plus starting materials phases of Ni and Al are present in the system while it seems that NiO is mainly consumed. Therefore, the sudden increase in temperature in addition to the formation of reaction products indicate that around 110 min of ball milling mechanically induced self-propagating reactions (MSR) has happened.

To compare the temperature difference caused by the occurrence of the exothermic reaction between raw materials in theory with in experimental observation, for which the temperature indicating strips indicated 5 °C increment, some assumptions are made. It is assumed that: 1) The reaction between raw materials has occurred completely,

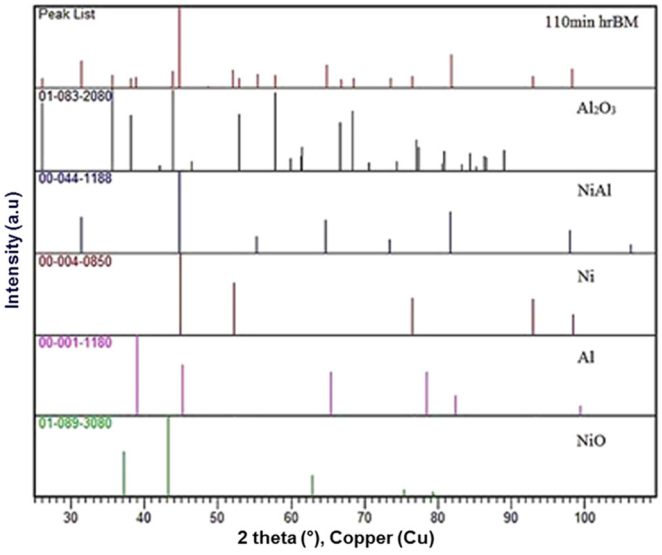

Fig. 4. XRD pattern of ball milled powder for 110 min and standard diffraction cards of predicted existing phases (NiO diffraction lines are reported just for comparison).

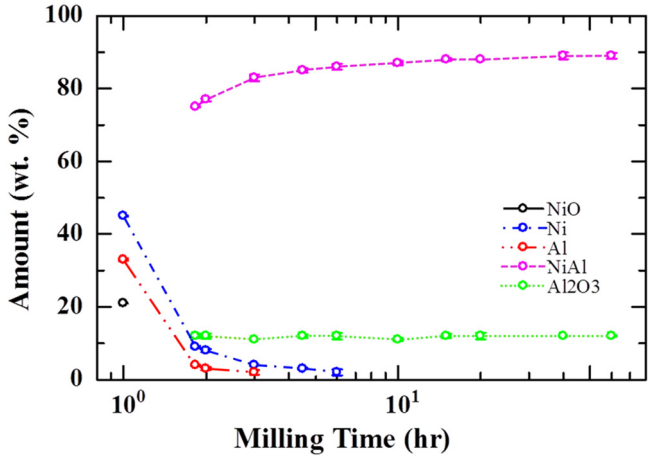

Fig. 5. Weight percentage of phases versus ball milling time based on Rietveld refinement results on X-ray diffraction data, 1–60 h of milling. Starting the formation of NiAl and Al_2O_3 at 110 min, presence of NiO until 110 min, presence of Al until 3 h and Ni until 6 h of milling.

2) Since the reaction happens very fast, only the ball mill vial, balls and powder mixture inside the vial absorb the released heat.

The thermodynamic data which have been used in calculations have been extracted from reference [40]. The heat capacity of the powder mixture is calculated based on the mixture rule. The ball mill vial mass is 2950 g. Mass of the powder mixture in theory is $M = 8M_{Ni} + 3M_{NiO} + 3M_{Al} = 1044.56$ g. If the reaction happens completely between raw materials with stoichiometric composition according to Eq. (1), the released heat is calculated as follows in Eq. (3):

$$\Delta H_1(\text{Reaction}, 298\ \text{K}) = \Delta H_f(Al_2O_3, 298\ \text{K}) + 11\Delta H_f(\text{NiAl}, 298\ \text{K}) - 3\Delta H_f(\text{NiO}, 298\ \text{K}) = -2259\ \text{kJ} = -2.259000\ \text{J} \quad (3)$$

Since the mass of the raw materials inside the ball mill vial is m = 5.85 g, the released heat from reaction in powder mixture of raw materials inside the ball mill vial will be:

$$\Delta H_2(\text{Reaction}, 298\ \text{K}) = \Delta H_1(\text{Reaction}, 298\ \text{K}) \cdot m/M = -12651.4\ \text{J} \quad (4)$$

Considering the heat absorbing materials absorb heat released by the reaction according to Eq. (4), the temperature rise is estimated to be as follows:

$$\Delta T = \Delta H_2/(\Sigma m C_p) = 9.5\ ^{\circ}\text{C} \quad (5)$$

The small difference between the calculated ΔT in theory in Eq. (5) and the measured ΔT in experimental conditions of the present work indicates that the above-mentioned assumptions for ΔT calculations are appropriate.

Therefore, by the temperature change in ball mill vial and results of phase analyses in Fig. 2, occurrence of mechanically induced self-propagating reaction after 110 min of milling is approved. According to these findings, it seems that NiO has been reduced by Al completely and the reaction between Ni and Al has occurred. Because of the high speed of these reactions, it is not possible to define their priority.

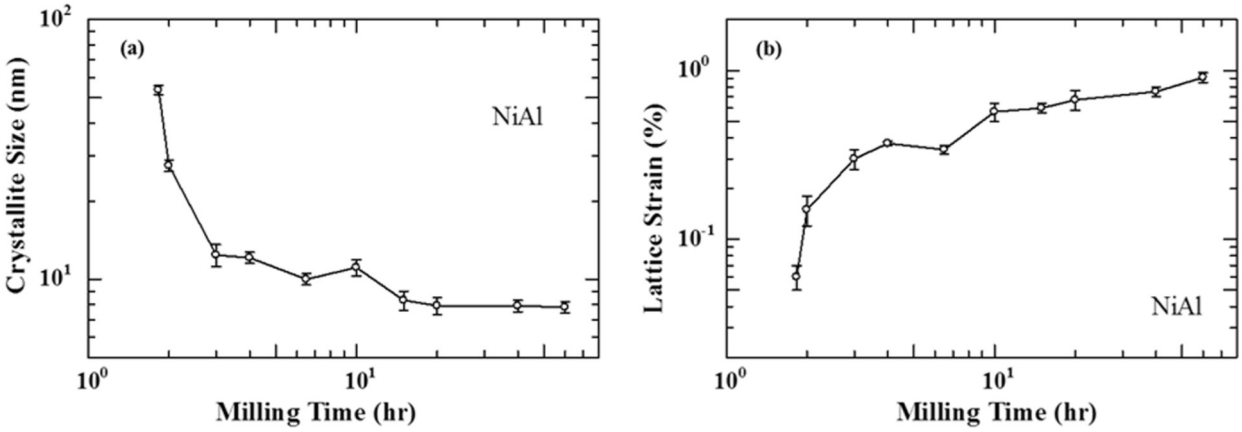

Fig. 6. Changes of (a) crystallite size and (b) lattice strain of NiAl phase with ball milling progression. NiAl formation starts at 110 min of milling.

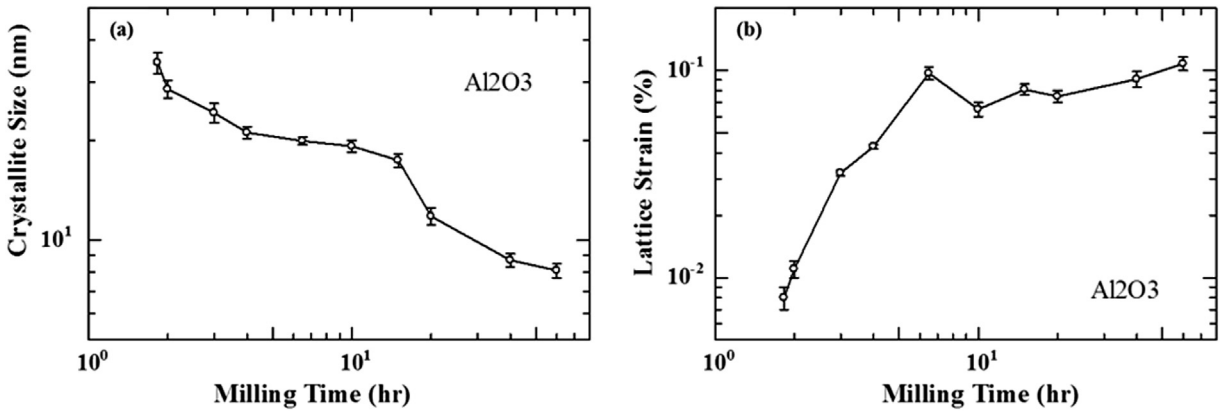

Fig. 7. Changes of (a) crystallite size and (b) lattice strain of Al_2O_3 phase with ball milling progression. Al_2O_3 formation starts at 110 min of milling.

While Udhayabanu et al. [41] observed that NiO reduction in the presence of Al happened gradually during milling. These researchers attributed the slow reaction rate of NiO reduction to wet milling in toluene medium. Toluene adheres on reactant particle surfaces, preventing them from reacting with each other. Also, these researchers observed γ-Al_2O_3 peaks by heating the 20 h ball milled powder to 900 °C and then α-Al_2O_3 peaks by heating to 1100 °C. They suggested that the amorphous alumina has formed in a substitution reaction because of fast heat dissipation in toluene medium.

3.3. Amount of existing phases with ball milling progression

Fig. 5 illustrates changes of the present phases' amount in the ball mill vial versus milling time based on results of quantitative analysis of Rietveld refinement. Ni, Al and NiO amounts in the mixed powder and have the same values as the ball milled powder for 1 h. After 110 min of ball milling and the occurrence of the exothermic reaction, NiO is mainly consumed and the aluminothermic reaction is relatively complete. Since the amount of Ni and Al shows a significant reduction, it seems that the NiAl observed in the powder sample is formed as a result of the reaction between Ni and Al in addition to the reaction between NiO and Al. By further milling, the reaction between Ni and Al continues and so the amount of Ni and Al decreases and more NiAl and Al_2O_3 product phases form. After 10 h of ball milling, only product phases are present in the sample. Calculation of weight percent of products according to stoichiometric reaction in Eq. (1) indicates that in the final sample there should be 9.8 wt% of Al_2O_3 and 90.2 wt% of NiAl in theory. Results of Rietveld refinement calculations in Fig. 5 indicate that the 10 h ball milled sample is composed of 11.4 ± 0.4 wt% of Al_2O_3 and 88.6 ± 0.6 wt% of NiAl. This slight difference might be because of oxidation during milling in air atmosphere.

3.4. Changes of crystallite size and lattice strain with milling time

Crystallite size and lattice strain of product phases in Figs. 6 and 7 are assessed by the Rietveld refinement method. The first data point refers to 110 min. It seems that the occurrence of the exothermic reaction at 110 min of milling causes the formed nuclei to grow in a fraction of second; crystallite size of NiAl and Al_2O_3 after 110 min of milling is 34 and 53 nm, respectively.

It can be seen in Figs. 6(a) and 7(a) that as expected with increment in ball milling time, the crystallite size of the phases decreased. Both figures demonstrate that the rate of decrease in crystallite size is very high during the early stages. The reason for this outcome can be explained as follows: at early stages of ball milling, intensive stresses lead to an increase in dislocation density which gradually results in the formation of regions with high dislocation density inside the grains. By milling prolongation and so increment in lattice strain, the crystal disintegrates into sub-grains which are separated by low-angle grain boundaries to lower the strain. Thus, decreasing the effective size in the crystalline region or crystallite refinement is the dominant mechanism during milling [7]. With continued milling, the rate of crystallite size reduction decreases over time until a steady state is achieved. This steady state variation is because of the contribution of more than one mechanism simultaneously. By the increase in crystal defect density, local temperature rises. So recrystallization and growth become active which result in grain growth. Finally, competition between plastic deformation via dislocation motion, which tends to decrease grain size, and the recovery and recrystallization behavior of the material, which tends to increase grain size, determines the final grain size.

As observed in Figs. 6(b) and 7(b), internal lattice strain of the phases increases at all times, but its increment rate reduces by progression in ball milling. The main reason for the accumulation of such strains is the stress localized by increasing density of dislocations and other lattice defects by milling [7]. As mentioned, by progression in milling and activation of recovery and recrystallization mechanisms, increment in lattice strain slows down [8]. Similar trends of changes of crystallite size and lattice strain with milling time has been reported by other researchers in reference [15,18].

Because of relatively low intensity of alumina peaks, calculations relating to this phase might have reduced accuracy. Sakaki et al. [42] and Bafghi et al. [43] in system of WC-Al_2O_3, expressed reduced accuracy in results relating to alumina because of low intensity of its peaks.

3.5. Chemical analysis of different phases by milling progression

Cross section of powder samples after different milling times (0, 1, 2, 6, 10, 20, 40 and 60 h) is investigated by SEM-BSE and EDS chemical analysis.

In Fig. 8, SEM micrograph of mixed powder and probable phases based on EDS analysis at different regions are shown. Raw materials

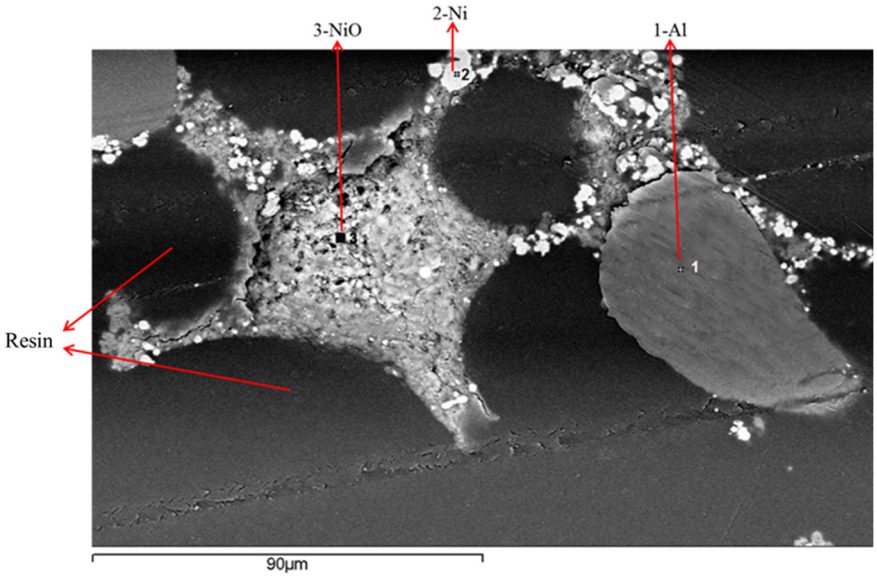

Fig. 8. SEM micrograph (BSE mode) of mixed powder and defining probable phases based on EDS analysis of different regions. Raw materials can be observed in this image.

can be observed in this image. Mixing of raw materials has not taken place completely and regions fully made of Ni and Al are distinguishable. Showing regions made of NiO phase was not easy because of smaller particle size of the primary NiO powder and since it is embedded in softer phases.

Fig. 9 shows SEM micrograph of powder ball milled for 1 h and its likely phases based on EDS analysis results at different regions. Also, EDS spectra of defined regions are presented in Fig. 9. Better mixing and further plastic deformation of raw materials can be seen in this image. Typical lamellar microstructure is observed in many regions nickel and nickel oxide particles are embedded in the soft aluminum during the ball milling process. EDS result shows that some areas are still composed of only nickel (region 1) and aluminum (region 2). In region 3, there is a mixture of nickel, aluminum and their oxides.

Fig. 10 shows SEM micrograph of powder ball milled for 2 h with probable phases at different regions based on EDS analysis results. Also, EDS spectra of defined regions are presented in Fig. 10. Regions 1 and 2 are composed of NiAl as the only phase. According to chemical analysis, it seems that region 3 is rich in aluminum and oxygen and region 4 is nickel-rich. These results are consistent with XRD results in Fig. 2, which showed that several phases existed in the powder milled for 2 h.

Fig. 11 reports SEM micrograph of powder ball milled for 6 h with probable phases corresponding to EDS analysis results. By milling progression to 6 h, existing phases are distributed more evenly in particles. According to the results of chemical analysis, regions 1 and 2 might be composed of NiAl. Region 3 seems to be rich in nickel and made of a nickel-rich phase. Region 4 is made of a mixture of NiAl and a high proportion of Al_2O_3.

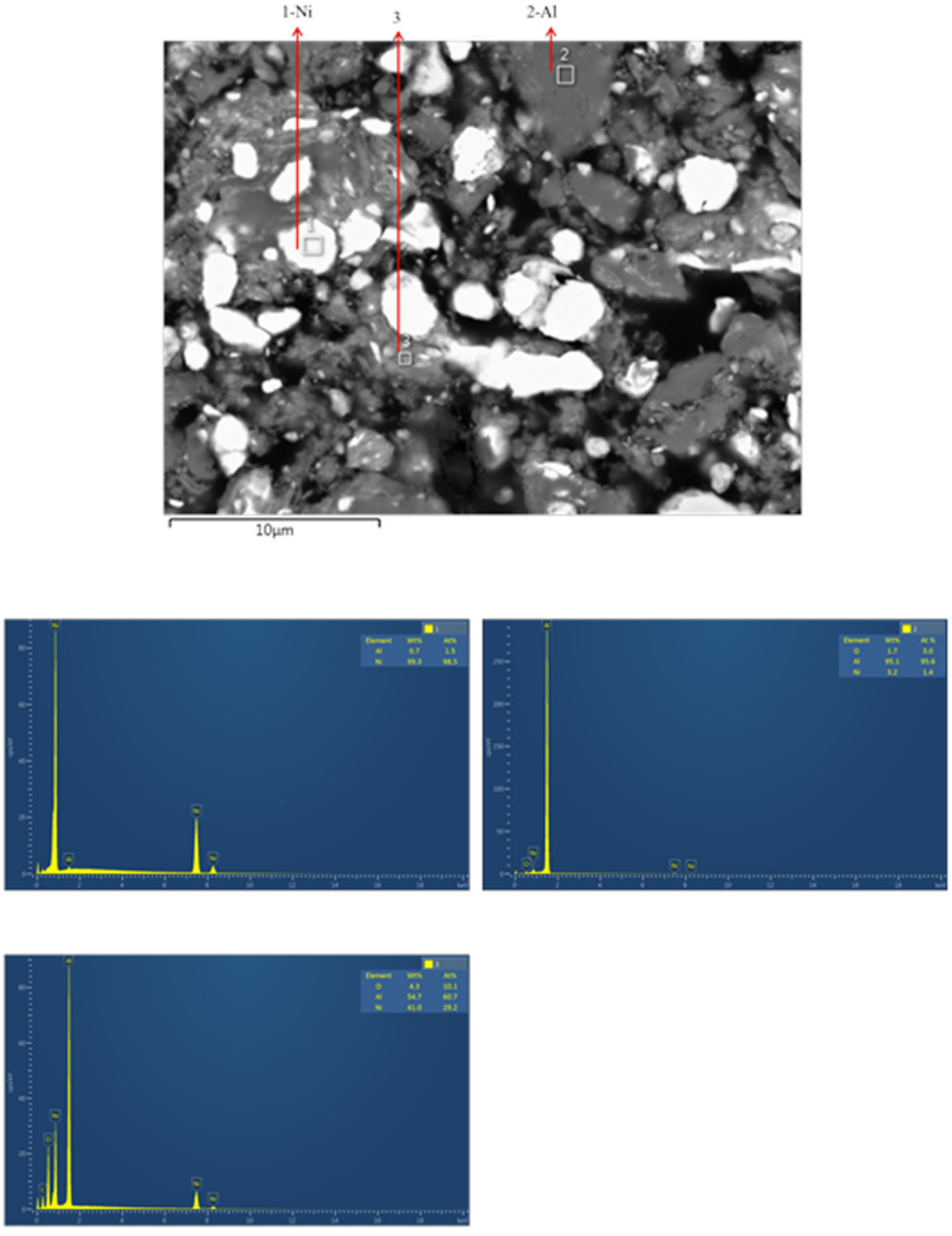

Fig. 9. SEM micrograph (BSE mode) of powder ball milled for 1 h and defining probable phases based on EDS analysis of different regions. EDS spectra of defined regions are presented. Better mixing and further plastic deformation of raw materials can be observed in this image.

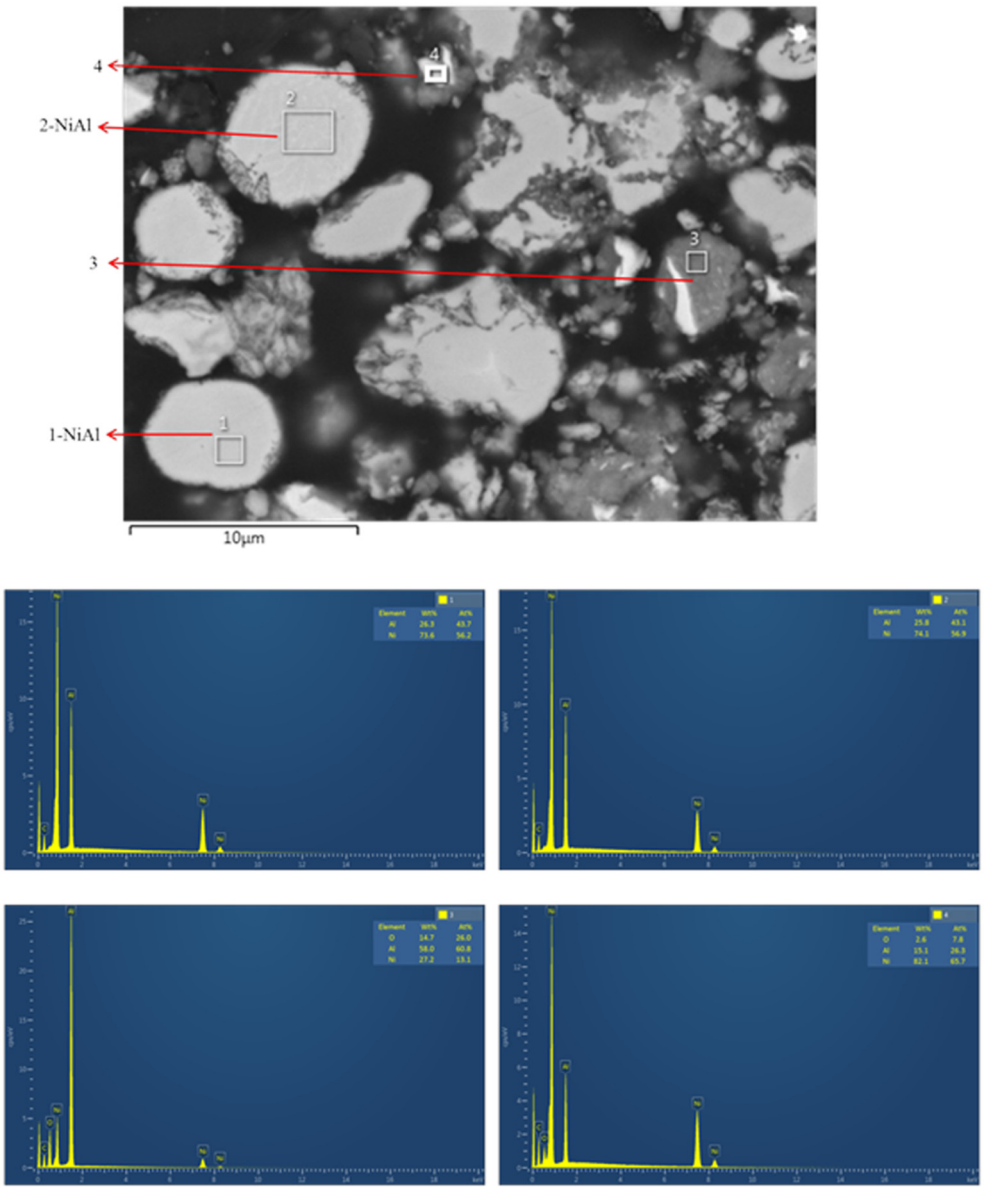

Fig. 10. SEM micrograph (BSE mode) of powder ball milled for 2 h and defining probable phases based on EDS analysis of different regions. EDS spectra of defined regions are presented. The reaction products are formed and raw materials still exist in this powder.

In Fig. 12, it is seen that after 10 h of ball milling, there are regions made of NiAl in addition to regions made of NiAl and Al_2O_3 mixture. These observations are consistent with XRD results for 10 h ballmilled sample in Fig. 3, which showed that only NiAl and Al_2O_3 exist in this sample. So, it is expected that by milling for more than 10 h, just microstructure refinement and more uniform distribution of the brittle component (Al_2O_3) in the ductile component (NiAl) may occur [7].

According to Fig. 13, after 20 h of ball milling the area of regions composed of just NiAl is decreased in comparison with the 10 h ball milled sample in Fig. 12 and microstructure develops towards more uniform Al_2O_3 distribution in NiAl matrix in powder particles. Results of chemical analysis show that iron impurity entered from ball mill vial to the powder.

By prolonging the milling, better mixture of two phases develops and Al_2O_3 is embedded in NiAl matrix to a greater extent. However, as seen in Fig. 14, even after 40 h of milling there are small regions like region 1 composed of only NiAl. In other places, uniform mixture of NiAl and Al_2O_3 is evolved. In Fig. 14, there is a very small white region composed of WC as a result of the entry of impurity from balls into the powder.

SEM micrograph and EDS results in different regions of powder milled for 60 h in Fig. 15 show that a uniform microstructure in the powder is achieved, and in all particles, Al_2O_3 is well distributed in the NiAl matrix. Fig. 15 (b) shows a powder particle with higher magnification which exhibits uniform distribution of dark gray phase in the matrix of light gray. Since this image is in BSE mode, dark gray areas seem to be rich in Al_2O_3 and light gray might be composed of NiAl.

3.6. Morphology of powder particles composed of NiAl and Al_2O_3 by milling progression

Fig. 16 shows powder particles from samples milled for 10, 20, 40 and 60 h. As can be seen in these images, after 10 h of milling, the morphology of powder particles is relatively spherical and such morphology

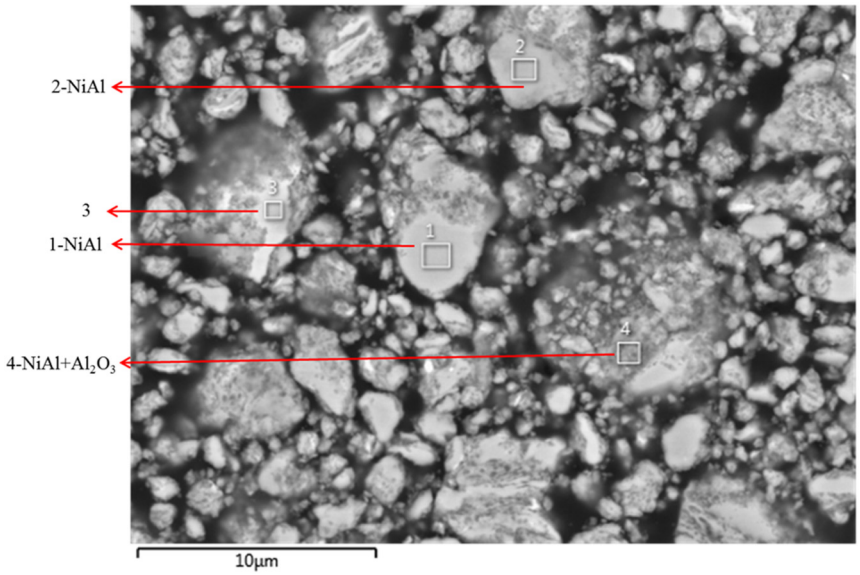

Fig. 11. SEM micrograph (BSE mode) of powder ball milled for 6 h and defining probable phases based on EDS analysis of different regions. Presence of reaction products as well as a small amount of residual nickel and more even distribution of phases in particles can be observed.

is also observed over longer times too. By increasing milling time, particle size decreases. Reduction in particle size in intermetallic-ceramic systems has been also reported in other references with NiAl-Al_2O_3 [23] and FeAl-Al_2O_3 [44] systems.

4. Conclusion

In the present work, the development of NiAl-Al_2O_3 nanostructured composite via a mechanochemical reaction in a powder mixtures of

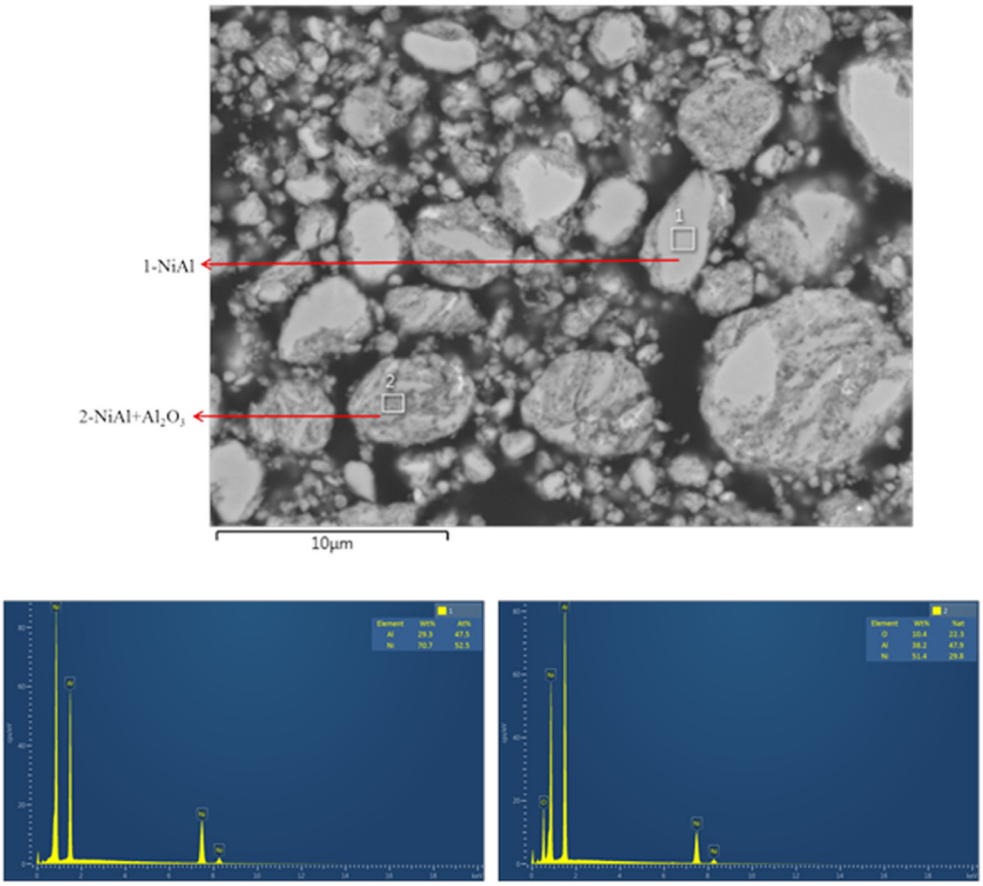

Fig. 12. SEM micrograph (BSE mode) of powder ball milled for 10 h and defining probable phases based on EDS analysis of different regions. EDS spectra of defined regions are presented. Only reaction products can be observed.

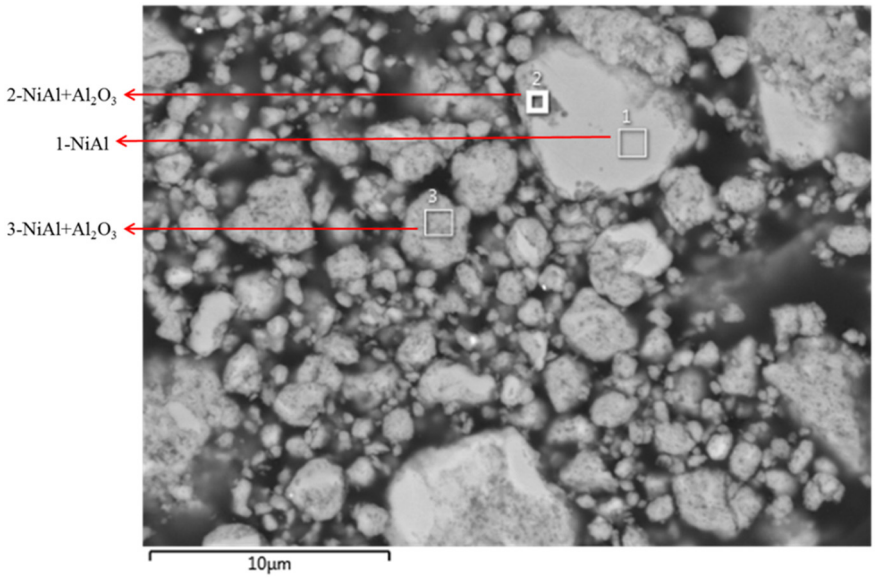

Fig. 13. SEM micrograph (BSE mode) of powder ball milled for 20 h and defining probable phases based on EDS analysis of different regions. Better distribution of Al_2O_3 in NiAl matrix in powder particles can be observed by milling progression.

13Al + 8Ni + 3NiO was investigated. The following conclusions can be derived from the experiments:

- In early stages of ball milling, that is up to 110 min, powder particles experienced mixing besides intense plastic deformation. This process caused layer-by-layer cold welding of phases on new and fresh surfaces of each other.
- For between 100 and 110 min of ball milling, a mechanically induced self-propagating reaction (MSR) took place. Ignition of the exothermic reaction caused a sudden temperature increase, NiO was consumed totally, the Ni and Al amount decreased and NiAl and Al_2O_3 as the reaction products phases were formed. Volume changes resulting from formation reaction of nickel aluminides were calculated. They showed that NiAl is the only phase which is expected to form in the system because of its highest volume reduction.
- By continuation of ball milling to 10 h, raw materials were no longer detected and just NiAl and Al_2O_3 existed in the ball mill vial. Increasing ball milling time to 60 h resulted in better intermixing of synthesized

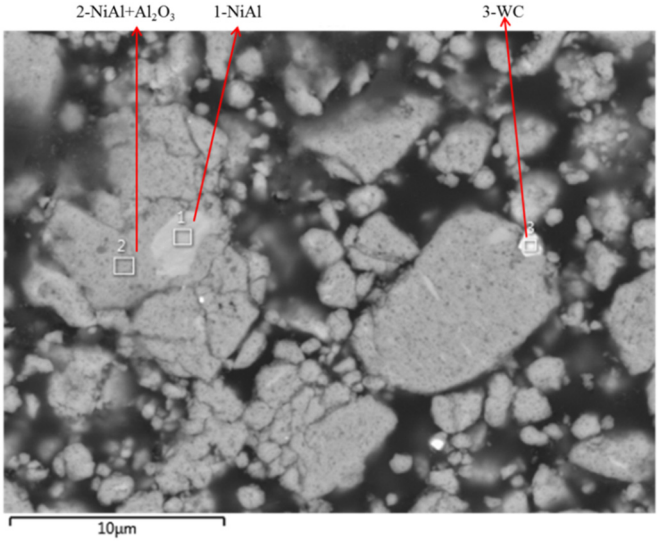

Fig. 14. SEM micrograph (BSE mode) of powder ball milled for 40 h and defining probable phases based on EDS analysis of different regions. Better distribution of Al_2O_3 in NiAl matrix in powder particles can be observed by milling progression.

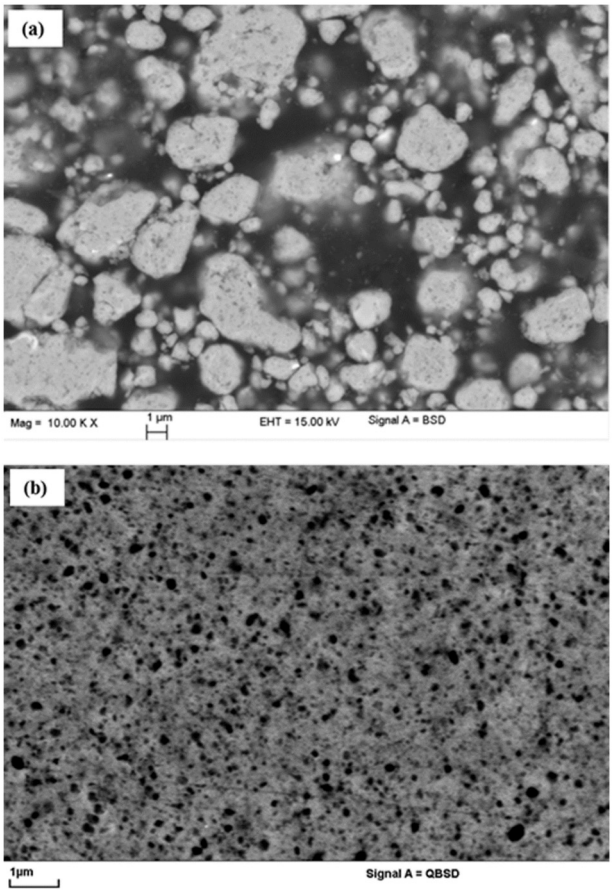

Fig. 15. SEM micrograph (BSE mode) of powder ball milled for 60 h, (a) lower magnification, (b) higher magnification, figures (a) and (b) are from two different regions of sample. These figures approve uniform distribution of Al_2O_3 in NiAl matrix.

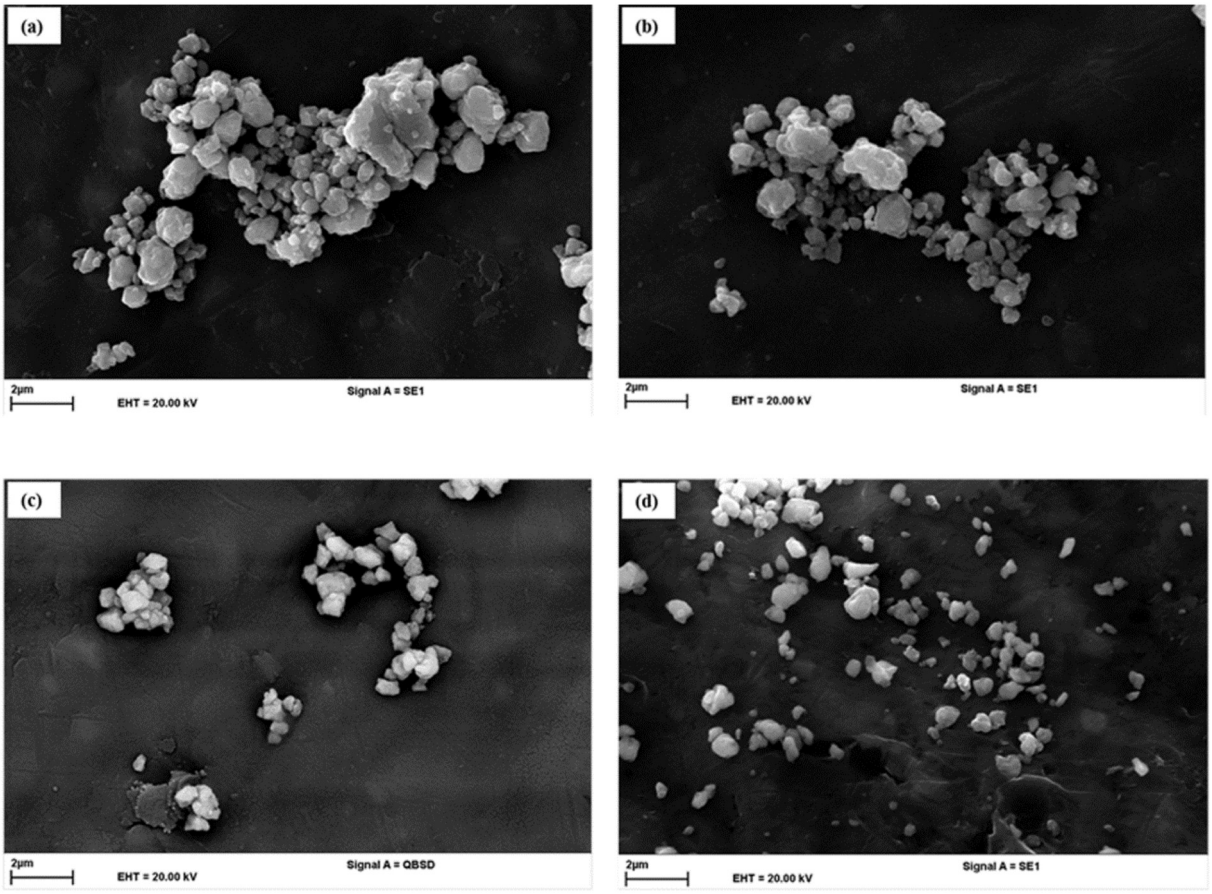

Fig. 16. SEM micrograph (SE mode) of powder particles milled for (a) 10 h, (b) 20 h, (c) 40 h and (d) 60 h. Relatively spherical morphology in different milling times and reduction in particle size is observed by milling prolongation.

phases, decrement in their crystallite sizes and increment in lattice strains, as well as decrement in powder particles size. Crystallite sizes of NiAl and Al_2O_3 were in nano-metric scale in all ball milling times, and after 60 h they both reached around 8 nm.

Acknowledgement

The authors would like to gratefully acknowledge the financial support provided for this project by the Ministry of Science, Research and Technology of Iran. We appreciate Professor Zhijian Shen's extensive help in providing the possibility of sample fabrication with ball mill apparatus in Department of Materials and Environmental Chemistry (MMK), Stockholm University. Also, we are grateful to Hans Bergqvist, senior researcher at R&D section of SWEREA-KIMAB for his generous scientific support and constant encouragement. We highly appreciate effective language help of Anthony Sloan, English assistant in National University of Ireland, Galway, Ireland.

References

[1] R. Jhajharia, D. Jain, A. Sengar, A. Goyal, P.R. Soni, Synthesis of copper powder by mechanically activated cementation, Powder Technol. 301 (2016) 10–15.
[2] M. Beyhaghi, A. Kiani-Rashid, M. Kashefi, J. Vahdati Khaki, S. Jonsson, Effect of powder reactivity on fabrication and properties of NiAl/Al_2O_3 composite coated on cast iron using spark plasma sintering, Appl. Surf. Sci. 344 (2015) 1–8.
[3] G. Chen, J. Chen, J. Peng, Effects of mechanical activation on structural and microwave absorbing characteristics of high titanium slag, Powder Technol. 286 (2015) 218–222.
[4] M. Beyhaghi, A. Kiani-Rashid, M. Kashefi, J. Vahdati Khaki, S. Jonsson, Investigation of in-situ synthesis and consolidation of NiAl–Al_2O_3 composites by reactive spark plasma sintering process using mechanically activated reaction, Int. J. Mater. Sci. Innovations 2 (2014) 100–116.
[5] E.T. Kubaski, O.M. Cintho, J.D.T. Capocchi, Effect of milling variables on the synthesis of NiAl intermetallic compound by mechanical alloying, Powder Technol. 214 (2011) 77–82.
[6] F. Hadef, Synthesis and disordering of B2 TM-Al (TM = Fe, Ni, Co) intermetallic alloys by high energy ball milling: a review, Powder Technol. 311 (2017) 556–578.
[7] C. Suryanarayana, Mechanical Alloying and Milling, Marcel Dekker, New York, 2004.
[8] C. Suryanarayana, Mechanical alloying and milling, Prog. Mater. Sci. 46 (2001) 1–184.
[9] A.S. Mukasyan, A.S. Rogachev, S.T. Aruna, Combustion synthesis in nanostructured reactive systems, Adv. Powder Technol. 26 (2015) 954–976.
[10] R. Ebrahimi-Kahrizsangi, M. Abdellahi, M. Bahmanpour, Ignition time of nanopowders during milling: a novel simulation, Powder Technol. 272 (2015) 224–234.
[11] M. Krifa, M. Mhadhbi, L. Escoda, J. Saurina, J.J. Suñol, N. Llorca-Isern, C. Artieda-Guzmán, M. Khitouni, Phase transformations during mechanical alloying of Fe–30% Al–20% Cu, Powder Technol. 246 (2013) 117–124.
[12] A. Biasetti, M. Meyer, L.M. Zélis, Hydriding kinetics of Mg-TiH_2 fine dispersions obtained by mechanosynthesis, Powder Technol. 307 (2017) 145–152.
[13] M. Slimi, M. Azabou, L. Escoda, J.J. Suñol, M. Khitouni, Structural and microstructural properties of nanocrystalline Cu–Fe–Ni powders produced by mechanical alloying, Powder Technol. 266 (2014) 262–267.
[14] B.S.B. Reddy, K. Rajasekhar, M. Venu, J.J.S. Dilip, S. Das, K. Das, Mechanical activation-assisted solid-state combustion synthesis of in situ aluminum matrix hybrid (Al_3Ni/Al_2O_3) nanocomposites, J. Alloys Compd. 465 (2008) 97–105.
[15] V. Udhayabanu, K.R. Ravi, B.S. Murty, Development of in situ NiAl–Al_2O_3 nanocomposite by reactive milling and spark plasma sintering, J. Alloys Compd. 509 (2011) S223–S228.
[16] E. Bahrami Motlagh, H. Nasiri, J. Vahdati Khaki, M.H. Sabzevar, Formation of metal matrix composite reinforced with Nano sized Al_2O_3+Ni–Al intermetallics during coating of Al substrate via combustion synthesis, Surf. Coat. Technol. 205 (2011) 5515–5520.
[17] D. Padmavardhani, A. Gomez, R. Abbaschian, Synthesis and microstructural characterization of NiAl-Al_2O_3 functionally gradient composites, Intermetallics 6 (1998) 229–241.
[18] H.X. Zhu, R. Abbaschian, In-situ processing of NiAl–alumina composites by thermite reaction, Mater. Sci. Eng. A 282 (2000) 1–7.
[19] G.H. Xu, Z. Lub, K.F. Zhang, The oxidation resistance of submicron-grained NiAl-Al_2O_3 composite fabricated by pulse current auxiliary sintering, Intermetallics 31 (2012) 99–104.

[20] W.W. Lee, D.B. Lee, M.H. Kim, S.C. Ur, High temperature oxidation of an oxide-dispersion strengthened NiAl, Intermetallics 7 (1999) 1361–1366.
[21] M. Beyhaghi, M. Kashefi, A. Kiani-Rashid, J. Vahdati Khaki, S. Jonsson, In-situ synthesis of nanostructured NiAl-Al_2O_3 composite coatings on cast iron substrates by spark plasma sintering of mechanically activated powders, Surf. Coat. Technol. 272 (2015) 254–267.
[22] C. Lin, S. Hong, P. Lee, Formation of NiAl-Al_2O_3 intermetallic-matrix composite powders by mechanical alloying technique, Intermetallics 8 (2000) 1043–1048.
[23] D. Oleszak, NiAl-Al_2O_3 intermetallic matrix composite prepared by reactive milling and consolidation of powders, J. Mater. Sci. 39 (2004) 5169–5174.
[24] K. Wieczorek-Ciurowa, K. Gamrat, NiAl/Ni_3Al–Al_2O_3 composite formation by reactive ball milling, J. Therm. Anal. Calorim. 82 (2005) 719–724.
[25] S.Z. Anvari, F. Karimzadeh, M.H. Enayati, Synthesis and characterization of NiAl–Al_2O_3 nanocomposite powder by mechanical alloying, J. Alloys Compd. 477 (2009) 178–181.
[26] V. Udhayabanu, K.R. Ravi, V. Vinod, B.S. Murty, Synthesis of in-situ NiAl-Al_2O_3 nanocomposite by reactive milling and subsequent heat treatment, Intermetallics 18 (2010) 353–358.
[27] M.J. Sayagués, M.A. Avilés, J.M. Córdoba, F.J. Gotor, Self-propagating combustion synthesis via an MSR process: an efficient and simple method to prepare (Ti, Zr, Hf)B2–Al_2O_3 powder nanocomposites, Powder Technol. 256 (2014) 244–250.
[28] M. Abbasi, S.A. Sajjadi, M. Azadbeh, An investigation on the variations occurring during Ni_3Al powder formation by mechanical alloying technique, J. Alloys Compd. 497 (2010) 171–175.
[29] R. Pretorius, A.M. Vredenberg, F.W. Saris, R.d. Reus, Prediction of phase formation sequence and phase stability in binary metal aluminum thin film systems using the effective heat of formation rule, J. Appl. Phys. 70 (1991) 3636–3646.
[30] E.G. Colgan, A review of thin-film aluminide formation, Mater. Sci. Rep. 5 (1990) 1–44.
[31] S.H.R.F. Nayeri, An Investigation on the Mechanism of TiC+Al_2O_3 Combustion Synthesis Via Mechanical Activation of Double Phases in TiO_2-Al-C SystemPhD thesis School of Metallurgy and Materials Engineering, Iran University of Science And Technology, 2006.
[32] P. Zhu, J.C.M. Li, C.T. Liu, Reaction mechanism of combustion synthesis of NiAl, Mater. Sci. Eng. A 329–331 (2002) 57–68.
[33] D.B. Miracle, The physical and mechanical properties of NiA1, Acta Metall. Mater. 41 (1993) 649–684.
[34] A.I. Popoola, Computational Study of Noble Metal AlloysPhD thesis The faculty of science, University of the Witwatersrand, 2013.
[35] M.H. Enayati, F. Karimzadeh, S.Z. Anvari, Synthesis of nanocrystalline NiAl by mechanical alloying, J. Mater. Process. Technol. 200 (2008) 312–315.
[36] V.K. Portnoya, A.M. Blinov, I.A. Tomilin, V.N. Kuznetsov, T. Kulik, Formation of nickel aluminides by mechanical alloying and thermodynamics of interaction, J. Alloys Compd. 336 (2002) 196–201.
[37] M. Atzmon, In situ thermal observation of explosive compound-formation reaction during mechanical alloying, Phys. Rev. Lett. 64 (1990) 487–490.
[38] M. Marashi, J. Vahdati Khaki, S.M. Zebarjad, Direct solid state synthesis of W–Al_2O_3 nanostructured composite using ammonium paratungstate (APT) and Al powder mixture, Int. J. Refract. Met. Hard Mater. 43 (2014) 13–18.
[39] A. Hoseinpur, M. Mohammadi Bezanaj, J. Vahdati Khaki, The effect of Al_2O_3 and CaO presence on the kinetics of mechanochemical reduction of MoS_2 by Zn, J. Alloys Compd. 587 (2014) 646–651.
[40] O. Kubaschewski, C.B. Alcock, P.J. Specner, Metallurgical Thermochemistry, Pergamon Press, New York, 1993.
[41] V. Udhayabanu, N. Singh, B.S. Murty, Mechanical activation of aluminothermic reduction of NiO by high energy ball milling, J. Alloys Compd. 497 (2010) 142–146.
[42] M. Sakaki, M.Sh. Bafghi, J. Vahdati Khaki, Q. Zhang, F. Saito, Conversion of W_2C to WC phase during mechano-chemical synthesis of nano-size WC–Al_2O_3 powder using WO_3–2Al–(1 + x)C mixtures, Int. J. Refract. Met. Hard Mater. 36 (2013) 116–121.
[43] M.Sh. Bafghi, M. Sakaki, J. Vahdati Khaki, Q. Zhang, F. Saito, Evaluation of process behavior and crystallite specifications of mechano-chemically synthesized WC–Al_2O_3 nano-composites, Mater. Res. Bull. 49 (2014) 160–166.
[44] J. Pourhosseini, M. Zakeri, M.R. Rahimipour, E. Salahi, G.R. Pourhosseini, Preparation of FeAl–Al_2O_3 nanocomposite via mechanical alloying and subsequent annealing, Mater. Sci. Technol. 26 (2010) 1132–1136.